On the Specimen Thickness Effect on Fatigue Crack Growth

Marco Antonio Meggiolaro
Jaime Tupiassú Pinho de Castro
Jorge Rodríguez Durán

Dept. of Mechanical Engineering, Pontifical Catholic University of Rio de Janeiro
Rua Marquês de São Vicente 225 – Gávea, Rio de Janeiro, RJ, 22453-900, Brazil
e-mails: meggi@mec.puc-rio.br, jtcastro@mec.puc-rio.br, duran@mec.puc-rio.br

Abstract
Crack closure is the most used mechanism to model thickness and load interaction effects on fatigue crack propagation. Based on it, the expected fatigue life of "thin" (plane-stress dominated) structures can be much higher than the life of "thick" (plane-strain dominated) ones, when both work under the same stress intensity range and load ratio. Therefore, if **da/dN** curves are measured under plane-stress conditions without considering crack closure, their use to predict the fatigue life of components working under plane-strain could lead to highly non-conservative errors. To avoid this error, it would be necessary to convert the measured crack growth constants associated with a given stress condition to the other using appropriate crack closure functions. However, crack closure cannot be used to explain some retardation effects after overloads on plane-strain fatigue crack growth. In this work, experimental evidence show that $\mathbf{\Delta K_{eff}}$ does not control the crack growth rate of some representative fatigue tests. These results indicate that the dominant role of crack closure in the modeling of the fatigue crack growth problem should be reviewed.

Keywords: Fatigue crack growth; Crack closure; Stress-state; Thickness effect

1. Introduction

It is a well-known fact that load cycle interactions can have a very significant effect in fatigue crack growth under variable amplitude loading. There is a vast literature proving that tensile overloads (OL), when applied over a baseline constant amplitude loading, can retard or even arrest the subsequent crack growth, and that compressive underloads can also affect the rate of crack propagation [1-7].

Neglecting these effects in fatigue life calculations can completely invalidate the predictions. In fact, when modeling many important fatigue problems, only after considering overload-induced retardation effects can the actual life reached by real structural components be justified. However, the generation of a universal algorithm to quantify these effects for design purposes is particularly difficult, due to the number and to the complexity of the mechanisms involved in fatigue crack retardation, among them plasticity-induced crack closure, blunting and/or bifurcation of the crack tip, residual stresses and/or strains, strain-hardening and/or strain-induced phase transformation, crack face roughness, and oxidation of the crack faces.

Besides, depending on the case, several of these mechanisms may act concomitantly or competitively, as a function of factors such as crack size, material microstructure, dominant stress-state, and environment. Moreover, the relative importance of the several mechanisms can vary from case to case, and there is so far no universally accepted single equation capable of describing the whole problem. Therefore, from the fatigue designer's point of view, load interaction ef-

fects must be treated in the most reasonably simplified way or, in Paris' wisdom words [1], its modeling must be kept simple.

But a simplified model must not be unrealistic, and so it is worthwhile mentioning that some simplistic models are unacceptable. For instance, it is not reasonable to justify the retardation effects by attributing to the overloads a significant variation in the residual stress-state at the crack tip. This is mechanically impossible: as the material near the crack tip yields in tension during the loading and in compression during the unloading of any propagating fatigue crack, there can be no significant variation in the residual stress state at the crack tip after an overload.

On the other hand, the main characteristic of fatigue cracks is to propagate cutting a material that has already been deformed by the plastic zone that always accompanies their tips. As discovered by Elber [8], fatigue crack faces are always embedded in an envelope of (plastic) residual strains and, consequently, they compress their faces when completely discharged, and open alleviating in a progressive way the (compressive) load transmitted through them, until reaching a load $\mathbf{P_{op} > 0}$, after which the crack is completely opened.

Elber's plasticity-induced crack closure is the most popular load interaction mechanism. It has long been proved to satisfactorily explain plane-stress load interaction effects [9]. In fact, neglecting crack closure in many fatigue life calculations can result in overly conservative predictions, increasing maintenance costs by unnecessarily reducing the period between inspections.

Even more important, according to some closure models, non-conservative predictions may arise from neglecting such effects. For instance, Newman [10-11] proposed that crack closure is not only a function of the load ratio **R**, but it is also dependent on the stress-state and on the maximum stress level. In this case, if plasticity-induced closure is the only mechanism affecting fatigue crack growth (FCG), the life of "thin" structures (in which FCG is plane-stress dominated) can be expected to be much higher than the life of "thick" ones (where FCG occurs under plane-strain dominant conditions), when both work under the same stress intensity range and load ratio. Therefore, if fatigue crack propagation curves are measured under plane-stress conditions without considering crack closure, then life predictions on components under plane-strain could lead to non-conservative errors as high as 75% according to Newman's model, see Fig. 1.

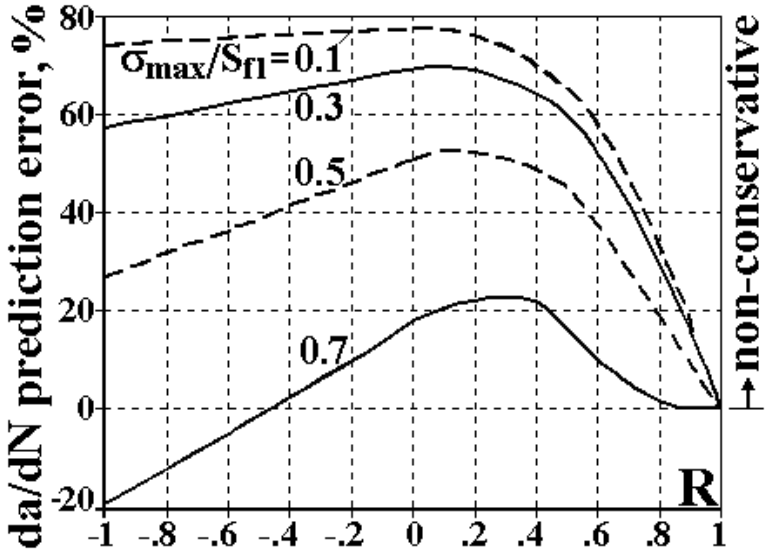

Fig. 1. Effect of the maximum stress σ_{max} and load ratio **R** on **da/dN** prediction errors for plane-strain calculations based on plane-stress data, according to Newman's closure function (Paris exponent 3.25).

To avoid this error, it would be necessary to convert the measured crack growth constants associated with a given stress condition to the other using appropriate crack closure functions. On the other hand, this thickness effect is not recognized by the ASTM E645 standard on the measurement of FCG rates (**da/dN**). In spite of mentioning the importance of crack closure, this standard only requires specimens sufficiently thick to avoid buckling during the tests.

This work presents experimental results on retardation effects after overloads on plane-strain FCG that cannot be explained by crack closure. These results indicate that the dominant role of crack closure on the modeling of fatigue crack growth should be reviewed.

2. Plasticity-induced crack closure

Elber [8] discovered that fatigue cracks only opened at a load $\mathbf{P_{op} > 0}$, because the plastic strains that surround them are compressed by the (elastic) residual ligament when it is unloaded, a phenomenon termed plasticity-induced fatigue crack closure. Experimentally, the compliance $\mathbf{C(a_0)}$ of a (plane) cracked body of thickness **t** and crack size $\mathbf{a_0}$ loaded by a force **P** can be calculated from its strain energy release rate $\mathcal{G} = (\mathbf{P^2/2t})\cdot(\mathbf{dC/da}) = (\mathbf{K_I})^2/\mathbf{E'}$ [7]:

$$\frac{dC}{da} = \frac{2tK_I^2}{P^2E'} = \frac{2t\sigma^2\pi}{P^2E'}\cdot[a\cdot f^2(a/w)] \;\therefore\; C(a_0) = \frac{2t\sigma^2\pi}{P^2E'}\int_0^{a_0}[a\cdot f^2(a/w)]\,da + C(0) \qquad (1)$$

where $\mathbf{C(0) = C(a_0 = 0)}$ is the uncracked body compliance, $\mathbf{K_I = \sigma\sqrt{(\pi a)}\cdot f(a/w)}$ is the stress intensity factor applied to the (cracked) body, σ is the applied stress, **a** is the crack size, **w** is the body width (or other characteristic dimension), and **E'** is Young's Modulus, with $\mathbf{E' = E}$ under plane-stress conditions or $\mathbf{E' = E/(1-\nu^2)}$ under plane-strain, ν being Poisson's ratio.

Figure 2 shows an example of a crack opening load $\mathbf{P_{op}}$ measurement during a fatigue crack propagation test. The opening load $\mathbf{P_{op}}$ is measured as the starting point of the linear part of the curve **P** versus **x**, where **x** is the displacement at the load application point (under linear elastic fracture mechanics conditions, **x** can be replaced by any proportional parameter, e.g. the crack mouth opening displacement δ or the back-face strain ε). It is worth mentioning that it is normally almost impossible to directly measure **x**, and that ε usually gives a cleaner signal than δ. Also, a circuit called the linearity subtractor [12] can be very helpful to improve the accuracy of $\mathbf{P_{op}}$ measurements. It is also important to point out that, in the authors' opinion, closure measurements based on global parameters like δ or ε are much more representative of the whole cracked body behavior than the local (or near crack tip) ones. These, being made on the body's surface, reflect its plane-stress behavior, which is not the dominant stress-state when FCG occurs in thick bodies.

In fact, the different behaviors caused by these surface effects have been verified from constant amplitude tests on center-cracked 10.2mm thick 2024-T3 aluminum plate specimens [13]. In these tests, a crack opening stress of 28% of the maximum stress σ_{max} was found under a stress ratio $\mathbf{R = 0.1}$. The specimens were then made thinner by removing surface layers at both sides of the plate specimens. After a thickness reduction to 7.7mm, the crack opening stress dropped to 13% of σ_{max}, and after a further thickness reduction to 3.75mm the result was 11% of σ_{max}. Because the major change in the opening stress was caused by the first thickness reduction, it is suggested that crack closure occurs predominantly near the material surface, under plane-stress conditions. Similar tests were performed by McEvily [14], using 6061-T6 aluminum compact specimens. In these tests, a typical crack growth retardation behavior was found after a 100% overload due to the developed crack closure, however when both specimen surfaces were ma-

chined away (reducing its thickness to half its original value) the retardation effect was largely eliminated.

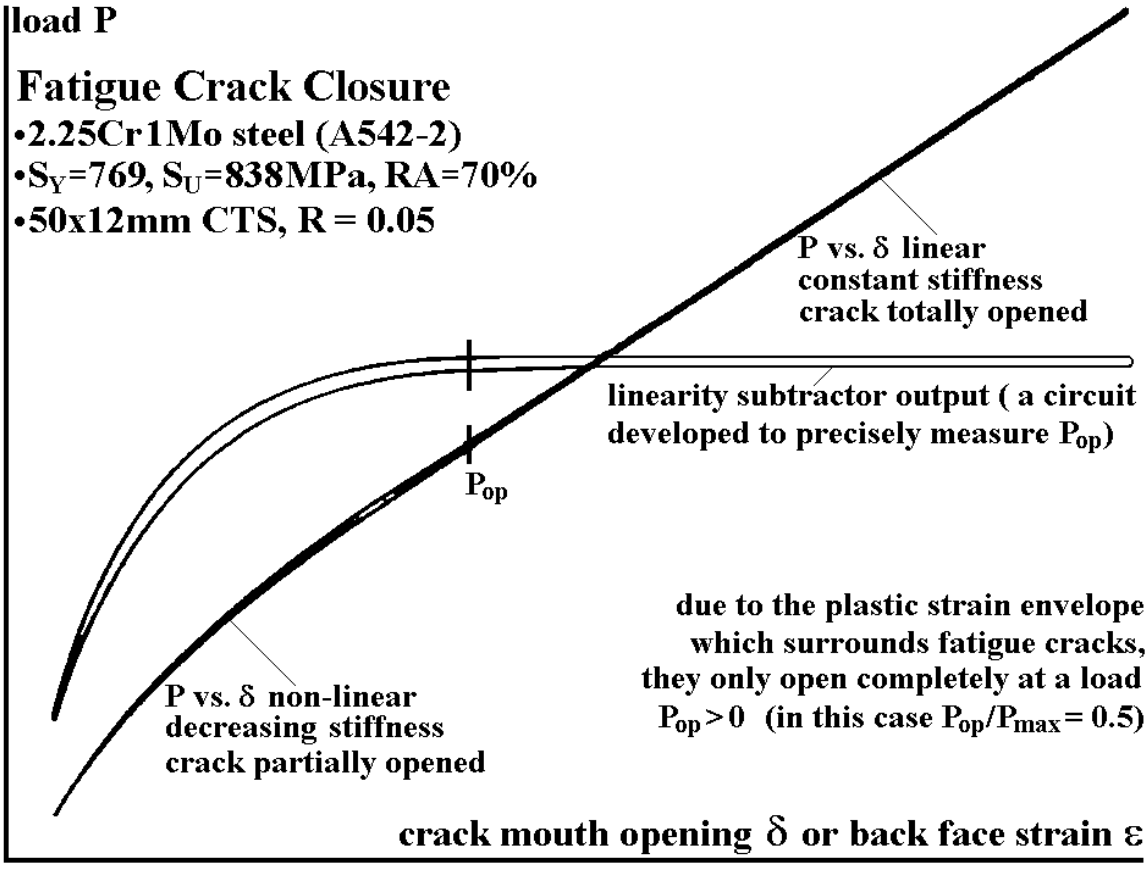

Fig. 2. Typical opening load measurement, including a linearity subtractor to enhance the non-linear part of the load **P** versus crack mouth **δ** or back face strain **ε**.

More crack closure near the surface agrees with the expected larger plastic zone sizes for plane-stress than for plane-strain. Paris and Hermann [15] suggested that fatigue cracks open first at mid-thickness and later at the material surface, therefore crack closure would be in fact a 3D phenomenon. As a result of more crack closure at the material surface, the crack front lags behind where it intersects the material surface, leading to curved crack fronts for through cracks in very thick specimens. Experiments on a 75 mm thick steel specimen under constant amplitude loading showed a crack front curvature with a lagging of 6.8 mm at the surface if compared to its mid-thickness plane-strain front [16]. However, such lagging is hardly observed in thinner specimens.

It might be stated that crack closure is predominantly a surface phenomenon occurring under plane-stress conditions. Since plastic deformations do not result in volume change, any plastic elongation in the loading direction must be compensated by a negative plastic strain in the thickness direction, which indeed occurs at the material surface. However, under pure plane-strain conditions, the strain in the thickness direction is zero, making it impossible to develop residual tensile strains at the crack faces, unless compressive plastic strains were to be found in the crack growth direction, which is not observed in practice [17].

To quantify the effects of crack closure, Elber [8] attempted to describe, with the aid of a physical model, the connection between load sequence, plastic deformation (by way of crack closure), and crack growth rate. He assumed that crack extension could not take place under cyclic

loads until it was fully opened, because only when $P_{op} > 0$ would the crack tip be stressed. Therefore, the bigger P_{op} and the corresponding K_{op}, the less would be the effective stress intensity range $\Delta K_{eff} = K_{max} - K_{op}$, and this ΔK_{eff} instead of $\Delta K = K_{max} - K_{min}$ would be the fatigue crack propagation controlling parameter. Based on experiments on 2024-T3 aluminum, Elber proposed a modification to the Paris growth equation taking into account the crack closure concept:

$$\frac{da}{dN} = A \cdot (K_{max} - K_{op})^m = A \cdot (\Delta K_{eff})^m \tag{2}$$

where **A** and **m** are material constants, which should be experimentally measured.

The stress ratio **R** is defined as K_{min}/K_{max}, leading to $\Delta K = (1 - R) \cdot K_{max}$. As the crack stops (**da/dN** tends to **0**) when **ΔK** tends to ΔK_{th}, the propagation threshold, then if Elber's closure is the only crack arrest mechanism, it would be expected that ΔK_{eff} is dependent on **R** and also that $\Delta K_{th} = (1 - R) \cdot K_{op}$:

$$\frac{da}{dN} = A \cdot (\Delta K_{eff})^m = A \cdot \left(\frac{(K_{max} - K_{op}) \cdot (1 - R)}{1 - R} \right)^m = A \cdot \left(\frac{\Delta K - \Delta K_{th}}{1 - R} \right)^m \tag{3}$$

However, the above equation has been developed for positive stress ratios only. Walker and Chang [18] considered the effects of compressive loads ($R < 0$), but their original formulation did not include explicitly the effect of ΔK_{th}, so in this paper a modified version is proposed:

For $\Delta K > \Delta K_{th}$ and $R \geq 0$,

$$\frac{da}{dN} = A \cdot \frac{(\Delta K - \Delta K_{th})^m}{(1 - \overline{R})^p} \text{ , where } \overline{R} = \begin{cases} R, \text{ if } R < R^+ \\ R^+, \text{ if } R \geq R^+ \end{cases} \tag{4}$$

for $\Delta K > \Delta K_{th}$ and $R < 0$,

$$\frac{da}{dN} = A \cdot (K_{max} - \Delta K_{th})^m (1 + \overline{R}^2)^q \text{ , where } \overline{R} = \begin{cases} R, \text{ if } R > R^- \\ R^-, \text{ if } R \leq R^- \end{cases} \tag{5}$$

and for $\Delta K \leq \Delta K_{th}$,

$$da/dN = 0 \tag{6}$$

where **A**, **m**, **p** and **q** are experimentally measured constants, and R^+ and R^- are the cutoff values for positive and negative stress ratios. Walker and Chang used $R^+ = 0.75$ and $R^- = -0.5$ for the above equations. Note that the constant **q** must be determined from test data generated for specific negative stress ratios ($R < 0$). The threshold stress intensity factor range used in these models can be determined for any positive stress ratio $R > 0$ by an empirical equation:

$$\Delta K_{th} = (1 - \alpha_t R) \Delta K_0 \tag{7}$$

where ΔK_0 is the crack propagation threshold value of the stress intensity factor range obtained from $R = 0$ constant amplitude tests, and α_t is a material constant determined from test data with various stress ratios. Another expression for the variation of ΔK_{th} as a function of **R** ($R > 0$) was proposed by Forman and Mettu [19]:

$$\Delta K_{th} = (4/\pi) \cdot \Delta K_0 \cdot \arctan(1 - R) \tag{8}$$

However, Newman et al. [10, 11] concluded from Finite Element calculations that crack closure does not only depend on **R**, as proposed by Elber, but it is also dependent on the maximum stress level σ_{max}. They proposed a crack opening function **f**, defined as the ratio K_{op}/K_{max} between the crack opening and the maximum stress intensity factors at each cycle. This function depends not only on **R**, but also on the ratio between the maximum stress σ_{max} and the material flow strength S_{fl} (for convenience defined as the average between the material yielding and ulti-

mate strengths, $S_{fl} = (S_Y + S_U)/2$), and on a plane stress/strain constraint factor α, ranging from $\alpha = 1$ for pure plane-stress to $\alpha = 3$ for pure plane-strain:

$$f = \frac{K_{op}}{K_{max}} = \begin{cases} \max(R, A_0 + A_1 R + A_2 R^2 + A_3 R^3), & R \geq 0 \\ A_0 + A_1 R, & -2 \leq R < 0 \end{cases} \tag{9}$$

where the polynomial coefficients are given by:

$$\begin{cases} A_0 = (0.825 - 0.34\alpha + 0.05\alpha^2) \cdot [\cos(\pi \sigma_{max} / 2S_{fl})]^{1/\alpha} \\ A_1 = (0.415 - 0.071\alpha) \cdot \sigma_{max} / S_{fl} \\ A_2 = 1 - A_0 - A_1 - A_3 \\ A_3 = 2A_0 + A_1 - 1 \end{cases} \tag{10}$$

From the definition of Newman's closure function f, the effective stress intensity range ΔK_{eff} can be rewritten as

$$\Delta K_{eff} = (1 - f) \cdot K_{max} = \frac{1 - f}{1 - R} \Delta K \tag{11}$$

Substituting Eqs. (9-10) into (11), correlations between ΔK_{eff} and the stress ratio R can be obtained for the plane-stress ($\alpha = 1$) and plane-strain ($\alpha = 3$) conditions, assuming $\nu = 0.33$ and $\sigma_{max}/S_{fl} = 0.3$ which, according to [11], would be a mean value for typical specimens used in FCG tests:

$$\frac{\Delta K_{eff}}{\Delta K} = \begin{cases} 0.52 + 0.42R + 0.06R^2, & R \geq 0 \text{ (plane stress)} \\ (0.52 - 0.1R)/(1 - R), & -2 \leq R < 0 \text{ (plane stress)} \\ \min(1,\ 0.75 + 0.69R - 0.44R^2), & R \geq 0 \text{ (plane strain)} \\ (0.75 - 0.06R)/(1 - R), & -2 \leq R < 0 \text{ (plane strain)} \end{cases} \tag{12}$$

Another correlation between ΔK_{eff} and R was obtained by Schijve [20],

$$\Delta K_{eff} = \Delta K\ (0.55 + 0.35R + 0.1R^2) \tag{13}$$

Equation (13) is also based on the concept of fatigue crack closure, agreeing within 7% with Newman's predictions for the plane-stress case. If α is interpreted as a curve-fitting parameter, then a value $\alpha = 1.15$ would have a better agreement with Schijve's correlation, instead of assuming $\alpha = 1$. Also, in practice many specimens under pure plane-strain conditions according to ASTM E399 (which validates K_{IC} toughness tests) have in fact constraint factors α between **1.9** and **2.7**, instead of the theoretical value $\alpha = 3$ [11].

Figure 3 compares Eqs. (12) and (13) as a function of R. Note that the predicted closure effects are much smaller under plane-strain than under plane-stress conditions, and that Newman's closure function predicts no crack closure (and therefore $\Delta K_{eff}/\Delta K = 1$) under dominantly plane-strain conditions for stress ratios R roughly above **0.5**.

In addition, increasing σ_{max} reduces Newman's closure function, resulting in predictions of higher da/dN rates. Figures 4 and 5 compare effective stress intensity ranges predicted by Newman for plane-stress, $\Delta K_{eff,\,\sigma}$, and for plane-strain, $\Delta K_{eff,\,\varepsilon}$, under different stress levels σ_{max}/S_{fl}. Figure 6 shows that Newman's effective stress intensity ranges can assume very different values for plane-stress and for plane-strain, especially when σ_{max}/S_{fl} is low.

Based on the above expressions for the effective stress intensity range, Forman and Newman proposed the following fatigue crack propagation rule to model all three crack growth regimens, including the effect of the stress state through Newman's closure function [19]:

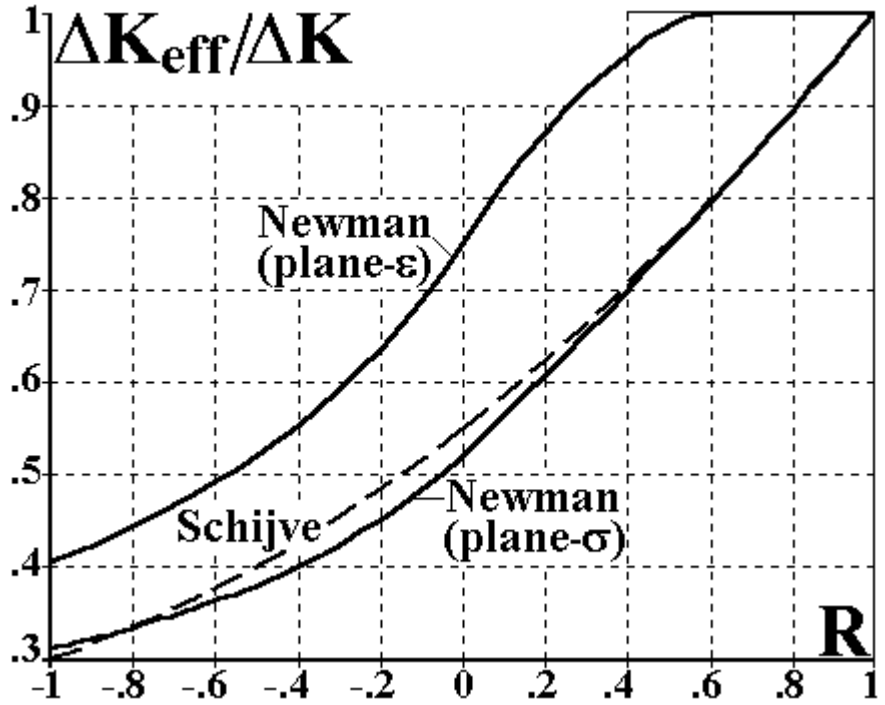

Fig. 3. Effective stress intensity ΔK_{eff} ranges as a function of the stress ratio **R**.

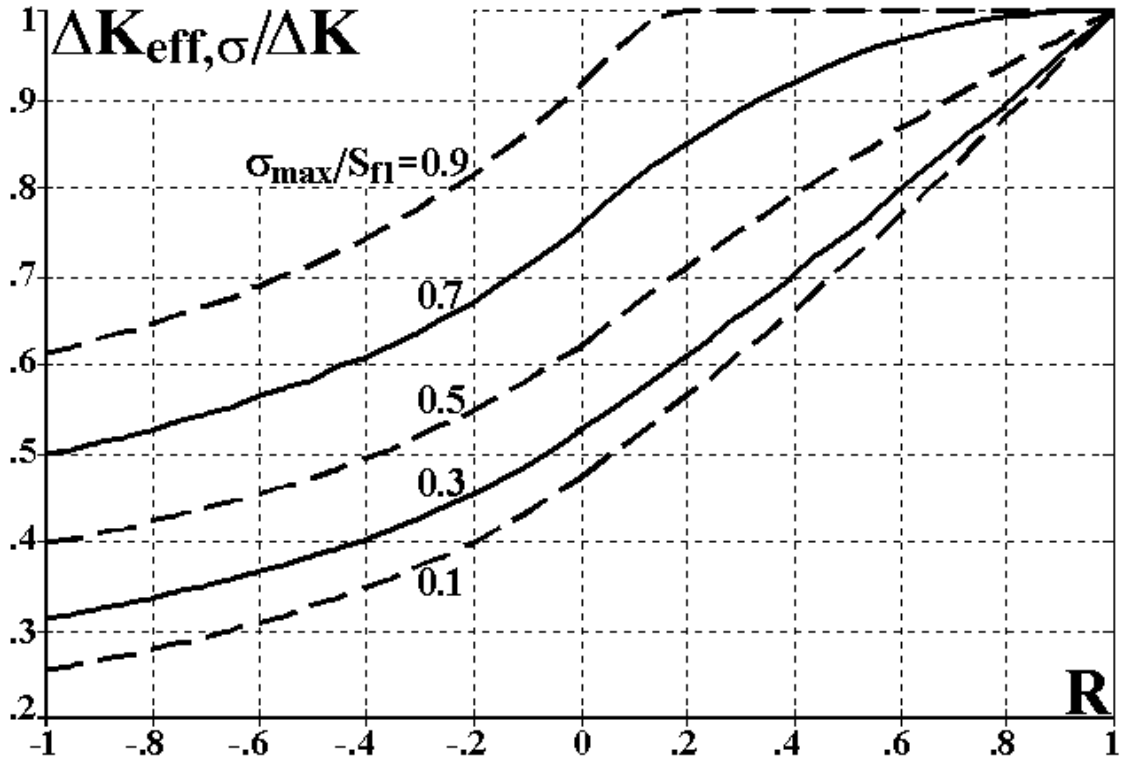

Fig. 4. Effect of σ_{max} on Newman's effective stress intensity range $\Delta K_{eff,\sigma}$ for plane stress.

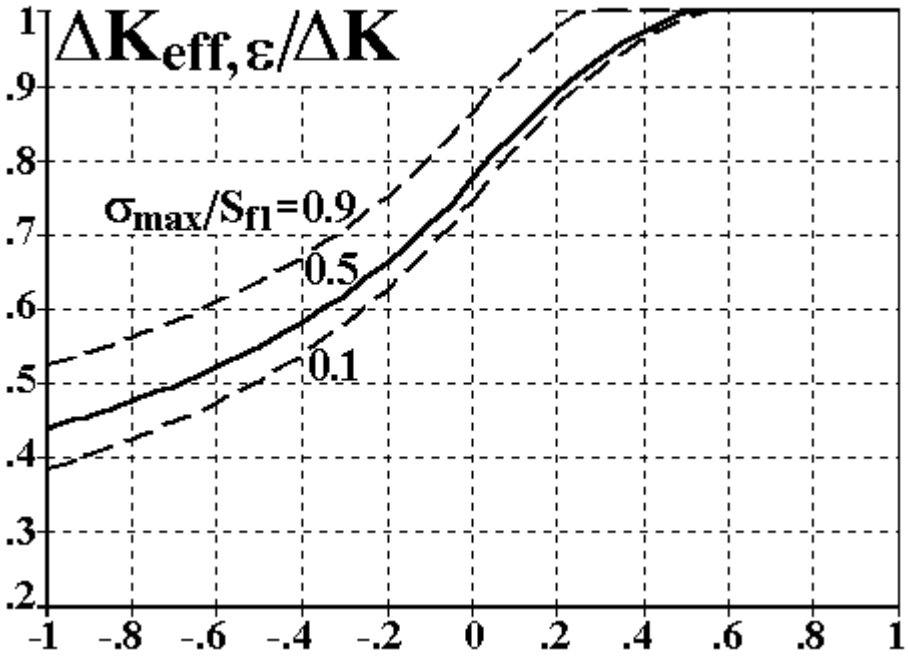

Fig. 5. Effect of σ_{max} on Newman's effective stress intensity range $\Delta K_{eff,\,\varepsilon}$ for plane strain.

$$\frac{da}{dN} = A \cdot \left(\frac{1-f}{1-R} \Delta K \right)^m \cdot \left(1 - \frac{\Delta K_{th}}{\Delta K} \right)^p \Bigg/ \left(1 - \frac{K_{max}}{K_C} \right)^q \tag{14}$$

where K_C is the critical (rupture) stress intensity factor, **A**, **m**, **p**, and **q** are experimentally adjustable constants.

Assuming that the fatigue crack growth rate is controlled by ΔK_{eff} instead of by ΔK (and, therefore, that plasticity induced closure is the sole mechanism which affects the propagation process), then the need for taking into account the stress-state in fatigue crack propagation tests must be emphasized. Consider, for instance, the effective stress intensity range ΔK_{eff} predicted by Newman for the plane-stress case when $R = 0$. In this case, according to Fig. 3, ΔK_{eff} is approximately equal to half the value of ΔK. This means that **da/dN** curves experimentally fitted to ΔK values without considering the crack closure effect would be actually correlating the measured **da/dN** rates with twice the actual (effective) stress intensity range acting on the crack tip. On the other hand, **da/dN** curves obtained in the same way ($R = 0$) under plane-strain conditions would be actually correlating **da/dN** with **4/3** of (and not twice) the effective stress intensity range. Therefore, one could not indiscriminately use crack growth equation constants obtained under a certain stress condition (e.g. plane-stress) to predict crack growth under a different state (e.g. plane-strain), even under the same stress ratio **R**.

Also, if a Paris **da/dN** vs. ΔK equation with exponent $m = 3.0$ (measured under plane-stress conditions and $R = 0$) is used to predict crack propagation under plane-strain, the predicted crack growth rate would be $[(4/3)/2]^m \approx 0.3$ times the actual rate, a non-conservative error of **70%**. Therefore, to avoid this (unacceptable) error, it would be necessary to convert the measured crack growth constants associated with one stress condition to the other using appropriate crack closure functions. Another approach would be to use in the predictions only **da/dN** vs. ΔK equations such as Eq. (14), which has already embedded the stress-state dependent closure functions.

This alarming prediction implies that the usual practice of plotting **da/dN** vs. **ΔK** instead of **da/dN** vs. ΔK_{eff} to describe fatigue crack growth tests would be highly inappropriate, because **da/dN** would also be a strong function of the specimen thickness **t**, which controls the dominant stress-state at the crack tip. Also, assuming that the classical ASTM E399 requirements for validating a K_{IC} toughness test could also be used in fatigue crack growth, plane-strain conditions would only apply if $t > 2.5(K_{max}/S_Y)^2$. In other words, one could expect to measure quite different **da/dN** fatigue crack growth rates when testing thin or thick specimens of a given material under the same **ΔK** and **R** conditions. Moreover, the concept of a "thin" or "thick" specimen would also depend on the load, since K_{max} increases with the applied stress. However, this thickness effect on **da/dN** is not recognized by the ASTM E645 standard on the measurement of fatigue crack propagation, which, in spite of mentioning the importance of crack closure, only requires specimens sufficiently thick to avoid buckling during the tests.

The errors associated with plotting **da/dN** vs. **ΔK** instead of ΔK_{eff} to predict crack growth under different stress states can be illustrated, e.g., using **m = 3.25** for the exponent of the Paris equation of an aluminum alloy. If data is measured under plane-stress conditions without considering crack closure, then the prediction under plane strain would be $(\Delta K_{eff,\sigma}/\Delta K_{eff,\varepsilon})^m$ times the actual rate, a non-conservative error of $[1 - (\Delta K_{eff,\sigma}/\Delta K_{eff,\varepsilon})^{3.25}]$. Using the ratio $\Delta K_{eff,\sigma}/\Delta K_{eff,\varepsilon}$ calculated from Newman's closure function (Fig. 6), this prediction error is plotted in Fig. 1 as a function of σ_{max} and **R**.

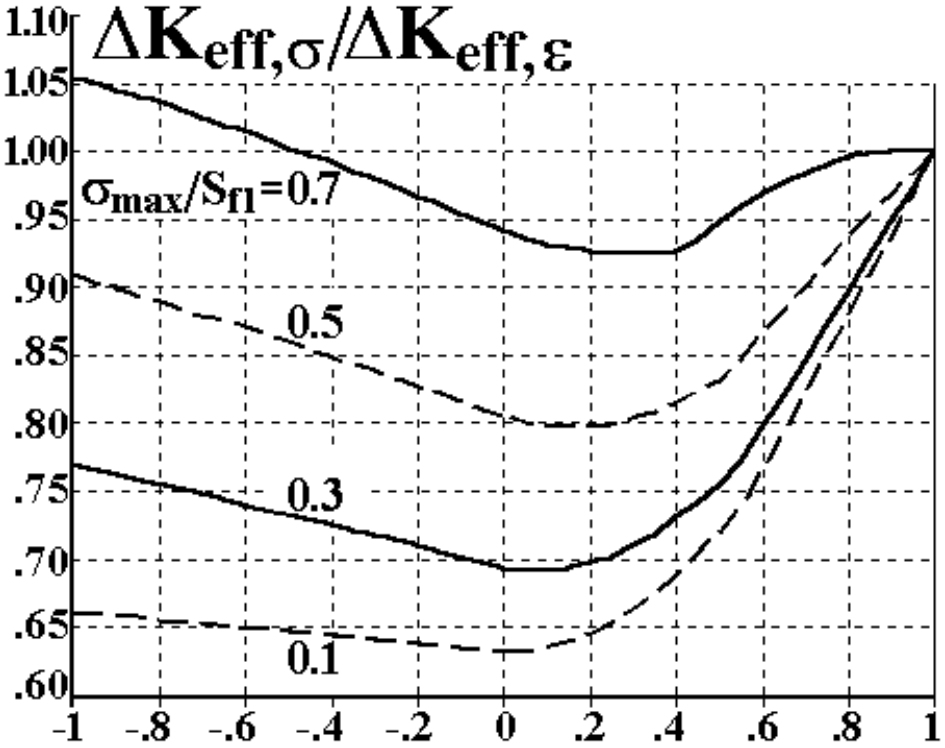

Fig. 6. Effect of σ_{max} and **R** on the ratio between Newman's effective stress intensity ranges for plane stress and plane strain, $\Delta K_{eff,\sigma}/\Delta K_{eff,\varepsilon}$.

In summary, since it is the thickness **t** the parameter that controls the dominant stress-state in FCG, one could expect the fatigue life of thin sheets (associated with larger plastic zones) to be

much higher than the life of thick plates (with smaller plastic zones), when both work under the same (initial) ΔK and R. One could also expect intermediate thickness structures, where the stress-state is not plane-stress nor plane-strain dominated, to have $1 < \alpha < 1/(1-2\nu)$ and a transitional behavior. Moreover, this transition can occur in the same specimen, if the crack starts under plane-strain and progressively grows toward a plane-stress dominated state. However, unlike the thickness effect on fracture toughness, the dominant stress-state usually is not object of much concern in fatigue design, but it certainly deserves a closer experimental verification.

On the other hand, it must be pointed out that many of the above results were derived from Finite Element calculations, and not from experimental measurements [10-11, 21]. It is a known fact that elastic-plastic FE calculations may offer significant problems due to non-linear aspects including material plasticity as well as changing contacts between the fracture surfaces during crack closure and opening [17]. In addition, the question whether plane-strain or plane-stress is applicable in the FE calculations is another problematic issue, essential to calculate the plastic zone sizes and therefore the plastic wake field of a crack.

Also, the FE models presented above assume that crack closure occurs everywhere near (and behind) the crack tip, including at the crack tip itself. However, Paris et al. [1] suggested that crack closure only occurs beyond a small distance d behind the crack tip, a phenomenon termed partial closure. Therefore, in an unloaded cracked body, the plastic strain wake around the crack faces would work as a wedge of thickness $2h$ that would cause a non-zero stress intensity of

$$K_{eff_{min}} = E'h/\sqrt{2\pi d} \tag{15}$$

To completely open the crack, releasing all compressive loads over the wedge, the crack opening displacement COD at a distance d of the crack tip must be equal to $2h$, therefore

$$COD = \frac{4K_{op}}{E'}\sqrt{\frac{2d}{\pi}} = 2h \Rightarrow K_{eff_{min}} = \frac{E'}{\sqrt{2\pi d}}\frac{2K_{op}}{E'}\sqrt{\frac{2d}{\pi}} = \frac{2}{\pi}K_{op} \tag{16}$$

It is interesting to point out that $K_{eff_{min}}$ does not depend on d or on $2h$. Therefore, from Eq. (16) it can be concluded that

$$\Delta K_{eff} = K_{max} - (2/\pi)K_{op} \tag{17}$$

would be the actual effective stress range under plasticity-induced crack closure conditions. This equation assumes that $K_{min} \le 0$, but if $0 < K_{min} \le K_{op}$, then

$$K_{max} - (2/\pi)K_{op} - (1-2/\pi)K_{min} \le \Delta K_{eff} \le K_{max} - (2/\pi)K_{op} \tag{18}$$

This ΔK_{eff} fitted well phase I of the da/dN curve of aluminum alloys, but its performance on phase II was a little bit disperse [1]. A better fitting was obtained substituting the constant $2/\pi$ by an adjustable parameter p, which varies from $p = 2/\pi$ close to ΔK_{th} until $p = 1$ in the Paris regime [22].

The partial closure model presented above shows the original crack closure concept in a somewhat different light. In addition, a closer survey of the literature reveals a series of test results that might even contradict some of the basic crack closure assumptions. When examining Ti6Al4V by the electropotential method, Shih and Wei [23] confirmed that crack closure depends on R and on K_{max}, which is in agreement with Dugdale's theory [24]. However, in that titanium alloy no crack closure was found for $R > 0.3$. According to Shih and Wei, neither the influence of R on the crack propagation nor the retardation effects can be completely explained by crack closure.

Bachmann and Munz [25] also conducted crack closure measurements on Ti6A14V, using an extensometer. However, unlike Shih and Wei, they were not able to discover any influence of $\mathbf{K_{max}}$ on crack closure behavior, which in turn would seem to confirm Elber's results.

Kim and Shim [11] found that the variance of **da/dN** is increased in thin specimens of 7075-T6 aluminum alloy, but no significant thickness dependence of the average **da/dN** rates was reported.

Other conflicting results have been found in the literature for tests under constant amplitude loading. Constant amplitude tests performed on compact tension (CT) specimens of 304 stainless steel with thicknesses varying between 3 and 25mm showed a relatively small thickness dependence [27]. It was found that the crack propagation rate on the 3mm specimen was 30% smaller than on the 25mm one, which is not much beyond the regular scatter of the experimental data. Costa and Ferreira [28] measured the growth rates on CT specimens of CK45 steel, with thicknesses varying between 6 and 24mm. It was found that the thickness dependence was only significant for low **R** ratios (**R < 0.2**) and low **ΔK** levels, while at **R = 0.4** constant amplitude loading no thickness effect could be observed. Such results might be explained either by different production techniques used to obtain the considered thicknesses (which could lead to different microstructures and therefore affect the growth rates), or simply by the fact that plasticity-induced closure may not be the main retardation mechanism in many cases, especially for higher **R** ratios.

On the other hand, tests under variable amplitude loading show a more systematic trend of increased retardation in thinner specimens. Crack growth retardation following an overload is usually dependent on the plastic zone size, which can be explained considering either crack closure or residual stress mechanisms. Thus, it should be expected that retardation effects are more intense in thinner specimens, which present larger plastic zones, as confirmed by tests performed by Mills and Hertzberg [29] on 2024-T3 aluminum specimens. It is also found that higher overload stress intensity levels result in increased retardation, which can be explained by a larger overload plastic zone.

A marked thickness effect under variable amplitude loading has also been found in tests performed by Saff and Holloway [30] on center-cracked specimens under a load spectrum based on F-4 aircraft loads. In these tests, the fatigue life of thick plates was found to be about 10 times shorter than for thin sheets. Results from Schijve [31] and Bernard et al. [16] showed the same trend. Shuter and Geary [32-33] performed single overload tests on CT specimens made of BS 4360 Gr.50D carbon-manganese steels, with thicknesses in the range 5-25mm. They suggested that there is a linear relationship between specimen thickness and the logarithm of the delay cycles. Also, crack retardation was found at baseline **R**-ratios as high as 0.5, even though no crack closure was detected at this **R** value. It has been suggested [3] that the plasticity induced crack closure mechanisms do operate at such high **R** ratios, however closure cannot be measured because the dimensional changes at the crack tip are too small to be detected by the mechanical compliance method. In opposition, Lang and Marci [5] claim that crack closure following an overload does not occur at high **R** values such as 0.5, and therefore crack closure can only play a secondary role. They attribute the retardation phenomenon primarily to the residual compressive stresses ahead of the crack tip after an overload. Another possible explanation could be due to crack path deflections and bifurcations [34-35], which can cause retardation even under high **R**-ratios due to the reduction in the stress intensity factor values caused by crack kinking. However, crack bifurcation has not been subject of much work in the literature. An extensive research program on crack bifurcation is now being conducted with the aid of a specialized Finite Element program called **Quebra2D** and a general purpose fatigue software named **ViDa** [36].

3. Experimental results

A comprehensive study on single overload effects in plane-strain fatigue crack growth was made in a tempered martensitic ASTM A-542/2 (2.25Cr1Mo) steel with yield and ultimate tensile strengths respectively $\mathbf{S_Y = 769}$ and $\mathbf{S_U = 838MPa}$, reduction in area **RA = 70%**, and hardness 23HRc, using 50×12.8mm CTS. Plane-strain conditions were enforced trying to maintain the OL plastic zone size much smaller than the specimen thickness **t**, or $\mathbf{zp_{OL} << t = 12.8mm}$, where the symbol "<<" was arbitrarily chosen in the ASTM E-399 standard sense, and in most experiments $\mathbf{t >> 2.5(K_{max}/S_Y)^2}$, $\mathbf{K_{max}}$ being the stress intensity factor associated to the OL peak.

The FCG tests were performed at two **R** ratios, **R = 0.05** and **R = 0.7**. The crack length was measured using a precise DC potential drop system, which had an uncertainty of 20μm [37]. The measured FCG curves of the A-542/2 steel at these two **R** ratios are shown in Fig. 7. Both **ΔK** increasing and **ΔK** decreasing data are shown in that figure. The 50Hz sinusoidal loads were applied under load control in a servo-hydraulic testing machine.

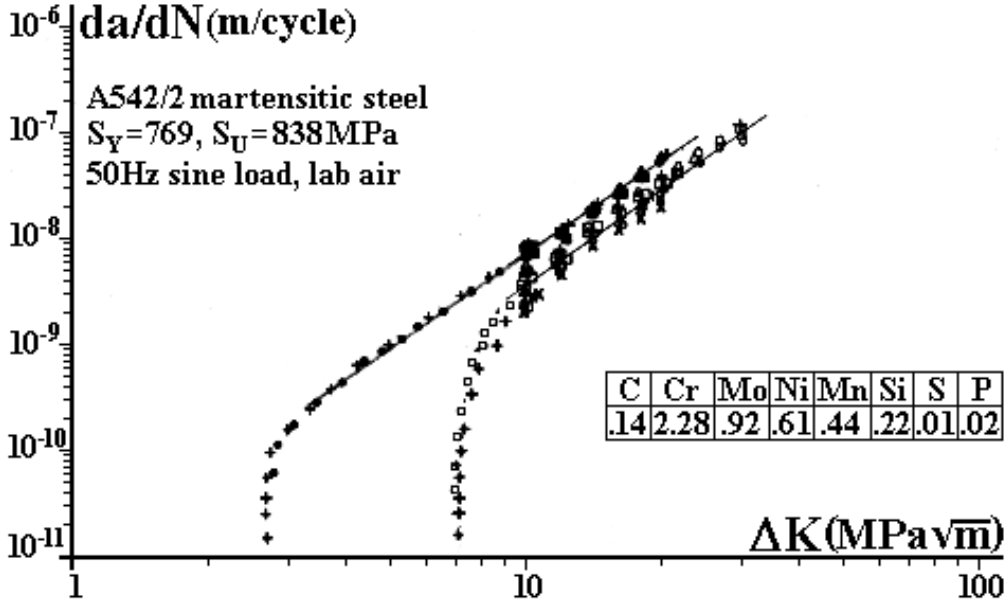

Fig. 7. A-542/2 steel **da/dN×ΔK** FCG curves at **R = 0.05** and **R = 0.7**.

All **R = 0.05** OL tests were made at a baseline (BL) stress intensity factor $\mathbf{\Delta K_{BL} = 10MPa\sqrt{m}}$, a point a little above the transition from phase I to phase II FCG. OL tests at **R = 0.7** were made at $\mathbf{\Delta K_{BL} = 8}$ or $\mathbf{\Delta K_{BL} = 10MPa\sqrt{m}}$, to obtain a BL FCG rate similar to the **R = 0.05** tests.

The (single) OL were slowly applied after stopping the test machine at the minimum baseline load, in order to be kept under close control. Special care was taken to avoid overshooting when restarting $\mathbf{\Delta K_{BL}}$ after completing the overload routine. Several OL could be applied in a same specimen, but always only after the effect of the previous one was completely overcome. This was assured by letting the BL FCG rate be regained and maintained for a crack increment several times larger than $\mathbf{zp_{OL}}$, the (maximum) OL plastic zone size.

As the maximum OL applied in the **R = 0.05** tests were 200%, it is found that in all these cases $\mathbf{zp_{OL} < 270\mu m}$ (assuming that $\mathbf{zp_{OL} = (1/2\pi)(K_{max}/S_Y)^2}$), which indeed was much smaller than the specimen thickness, justifying the plane-strain controlled FCG claim. In the **R = 0.7** tests, the maximum OL were 100%, and the corresponding $\mathbf{zp_{OL} = 1.2mm}$, a little larger than the E-399 requirement but still an order of magnitude below the CTS thickness.

An OL could have no detectable effect on the subsequent FCG rate, could delay the crack or even stop it, depending on its magnitude. Typical retardation results at **R = 0.05** and **R = 0.7** are shown in Figs. 8 through 11. Note that some curves in Fig. 11 are associated with negative cycles because the overload cycle was offset and defined as cycle zero. Overloads of 25% (or a 1.25 ratio between the OL and the BL peaks) have no detectable effects in both **R** ratios, while 100% OL at **R = 0.7** or 150% OL at **R = 0.05** always stopped the cracks. Also, increasing retardation was observed between these 100% and 150% values (crack arrest after a 134% OL at **R = 0.05** is shown in Fig. 10). The overall crack behavior in the OL affected zone was similar but not identical to the classical plane-stress one, since no delayed retardation was ever observed, and the size of the OL affected zone was generally smaller than $\mathbf{zp_{OL}}$.

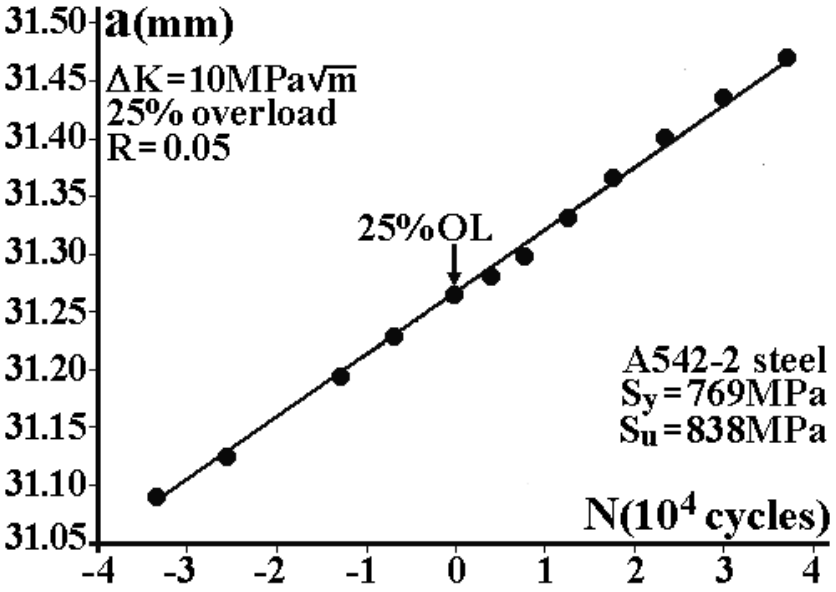

Fig. 8. No detectable crack retardation after a 25% overload, **R = 0.05**.

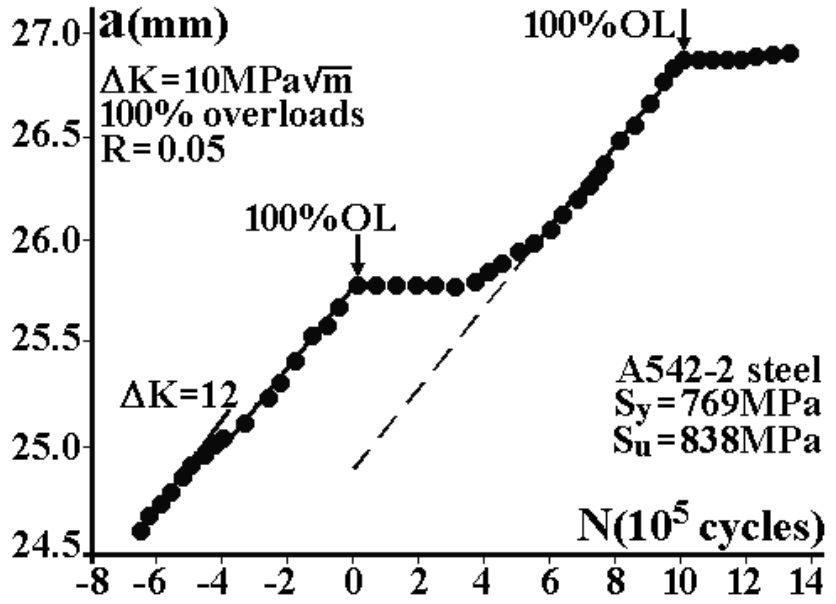

Fig. 9. Fatigue crack growth retardation after a 100% overload, **R = 0.05**.

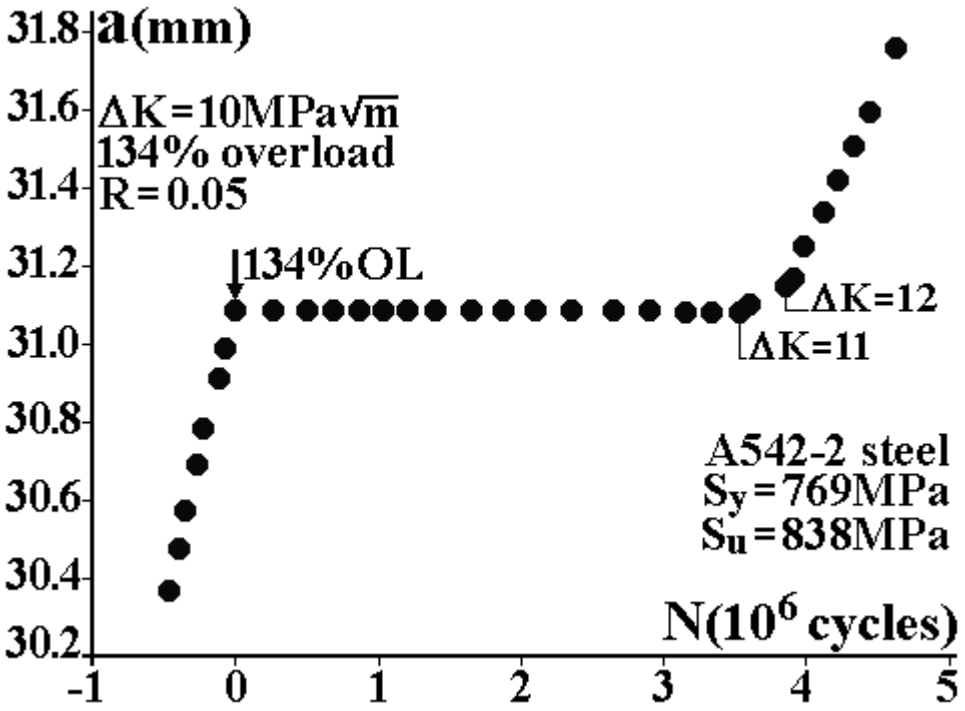

Fig. 10. Fatigue crack arrest after a 134% overload, **R = 0.05**.

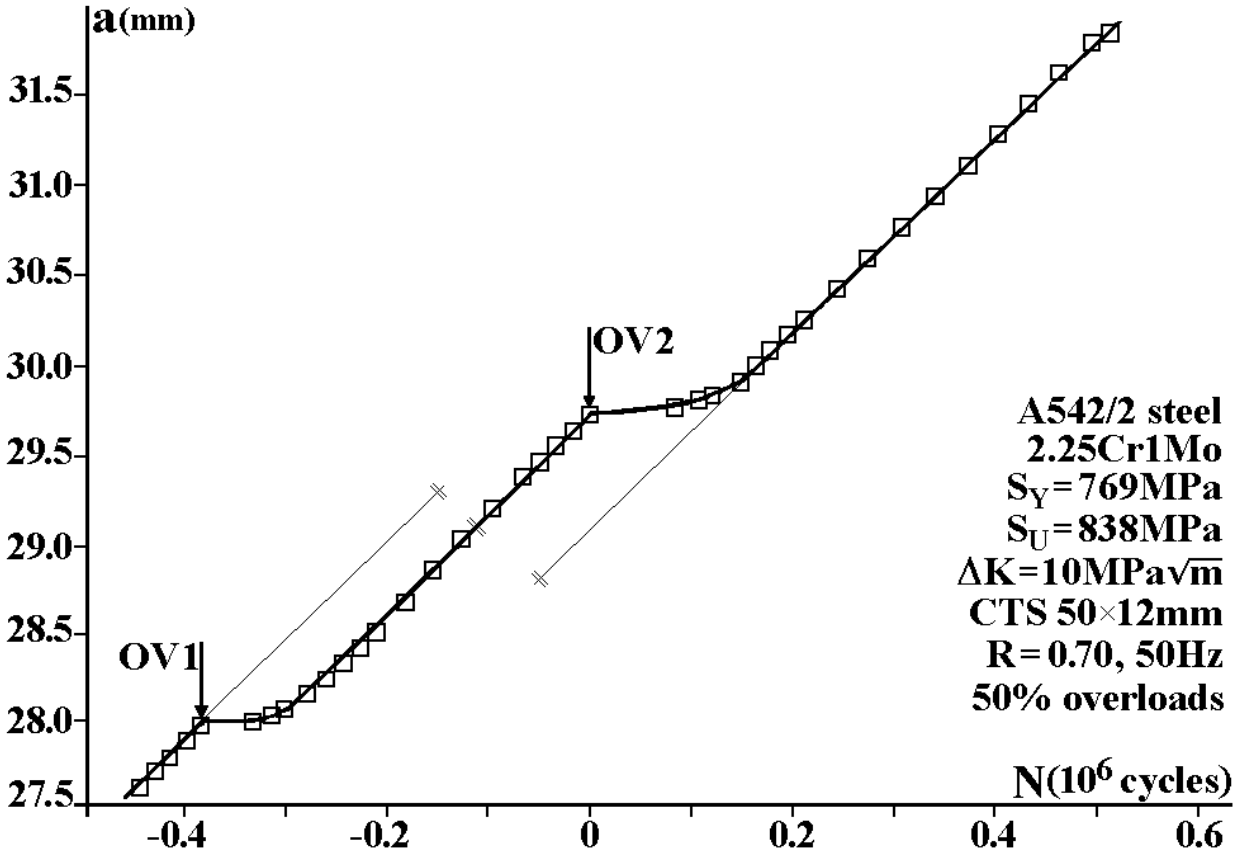

Fig. 11. Fatigue crack growth retardation after a 50% overload, **R = 0.7**.

Careful crack closure measurements were made before and after the overloads, in order to study its influence on the subsequent FCG behavior. These measurements were particularly precise, since their scatter in consecutive cycles was negligible, as illustrated in Fig. 12. This figure shows several $\mathbf{P \times \varepsilon}$ and $\mathbf{(P - k\varepsilon) \times \varepsilon}$ curves measured in subsequent load cycles. This last type of curve is the linearity subtractor output, were **k** is the slope of the linear part of the $\mathbf{P \times \varepsilon}$ curve, which was fitted by means of an analog differentiator, as described in [12]. The crack opening load $\mathbf{P_{op}}$ could then be easily identified, and a two-digit resolution on $\mathbf{P_{op}/P_{max}}$ measurements could be guaranteed. It must be pointed out that the various curves in Fig. 12 had to be displaced to enhance their individuality, otherwise they would be coincident. In all these measurements, $\mathbf{P_{op}/P_{max} = 0.28}$.

Figure 13 shows the closure measurements made just after the 100% OL was applied. Two very important features are evident from this figure. First, as in Fig. 12, the measurements are again very repeatable. Second, and much more important, the crack opening load ***decreased*** after the OL, since $\mathbf{P_{op}/P_{max} = 0.23}$ in this case. However, associated to this increase in $\mathbf{\Delta K_{eff}}$, no crack growth could be detected, and all $\mathbf{P_{op}}$ measurements in this period gave the same $\mathbf{P_{op}/P_{max} = 0.23}$ result, as shown in Fig. 14. Only after $7.5 \cdot 10^4$ cycles could the potential drop system sense a small increase in the crack size, associated to an ***increase*** in $\mathbf{P_{op}}$, which rose to $\mathbf{P_{op}/P_{max} = 0.25}$. Moreover, when the OL effect completely ceased, $\mathbf{P_{op}}$ returned to the value it had before the OL, see Fig. 15. This result, of course, is exactly the opposite of what would be expected if the overload-induced retardation was caused by a crack closure mechanism.

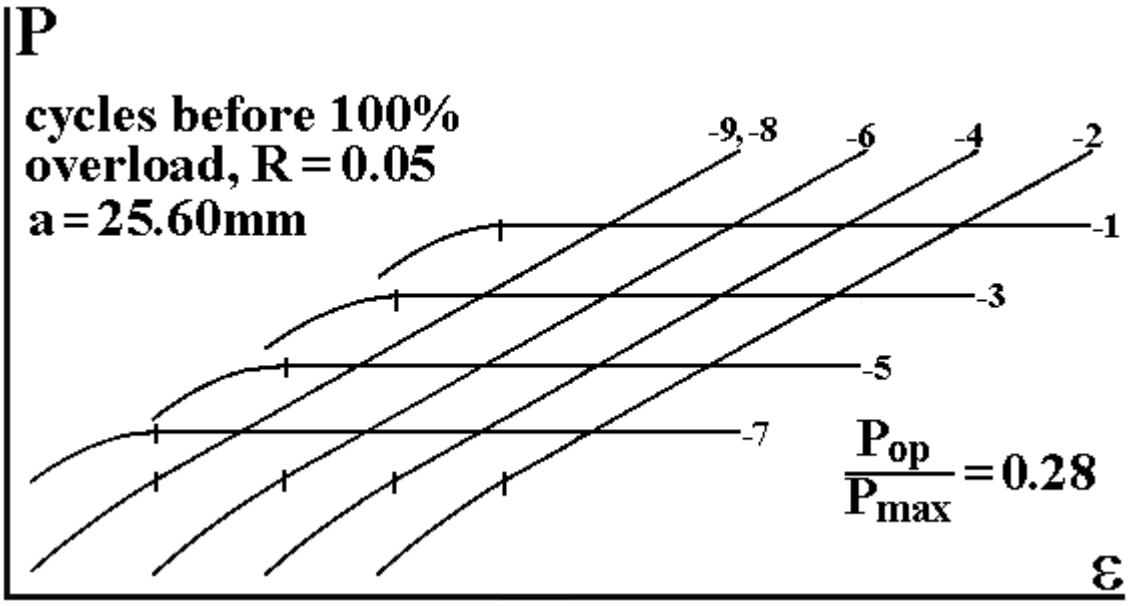

Fig. 12. Crack closure measurement before a 100% overload, **R = 0.05**.

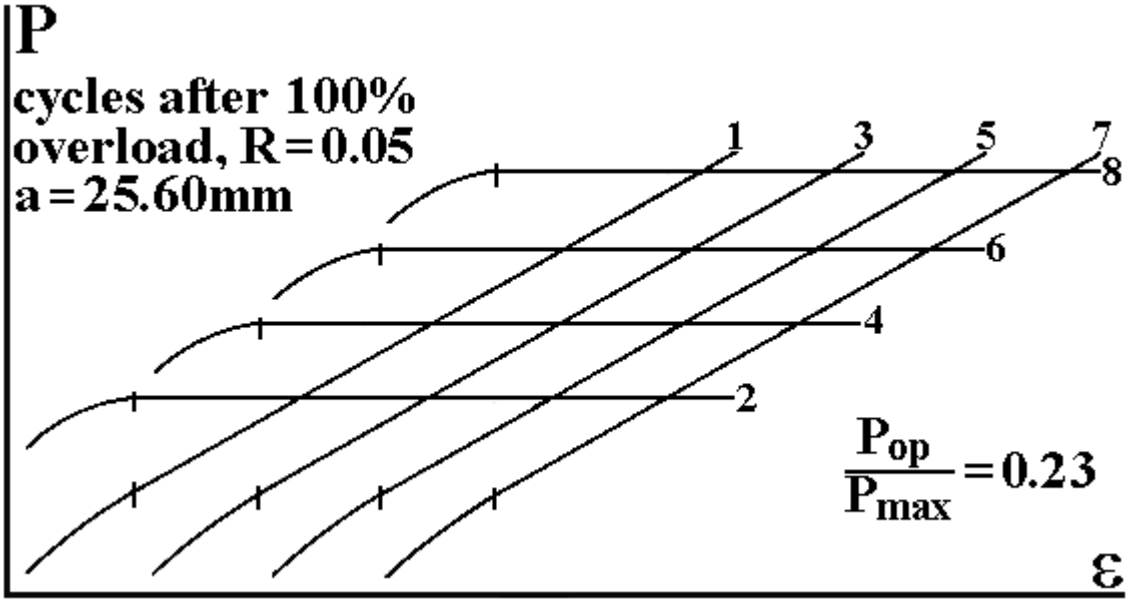

Fig. 13. Crack closure measurements just after the 100% OL reported in Fig. 12.

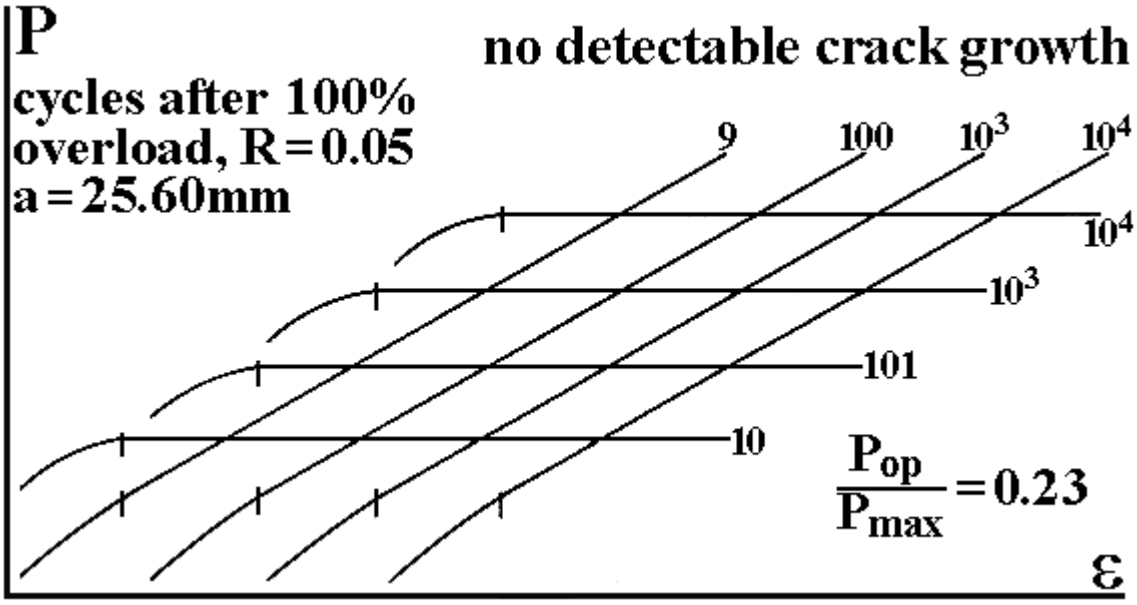

Fig. 14. Crack closure measurements with no detectable crack growth, despite the 22% ***increase*** in ΔK_{eff} after the 100% OL.

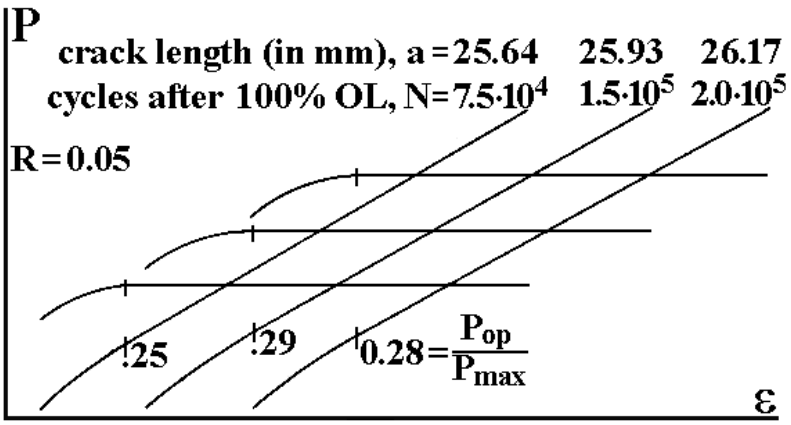

Fig. 15. Crack closure measurements after the overload, when P_{op}/P_{max} ***increased*** until reaching its previous value $P_{op}/P_{max} = 0.28$, when the OL effect ceased completely.

Exactly the same type of behavior has been reported a long time ago by Castro and Parks [35], in a more striking situation. As presented in Fig. 16, after a 200% OL the fatigue crack was arrested, despite the 31% ***increase*** in ΔK_{eff}. Again, an incompatible behavior was found with respect to ΔK_{eff}-controlled FCG.

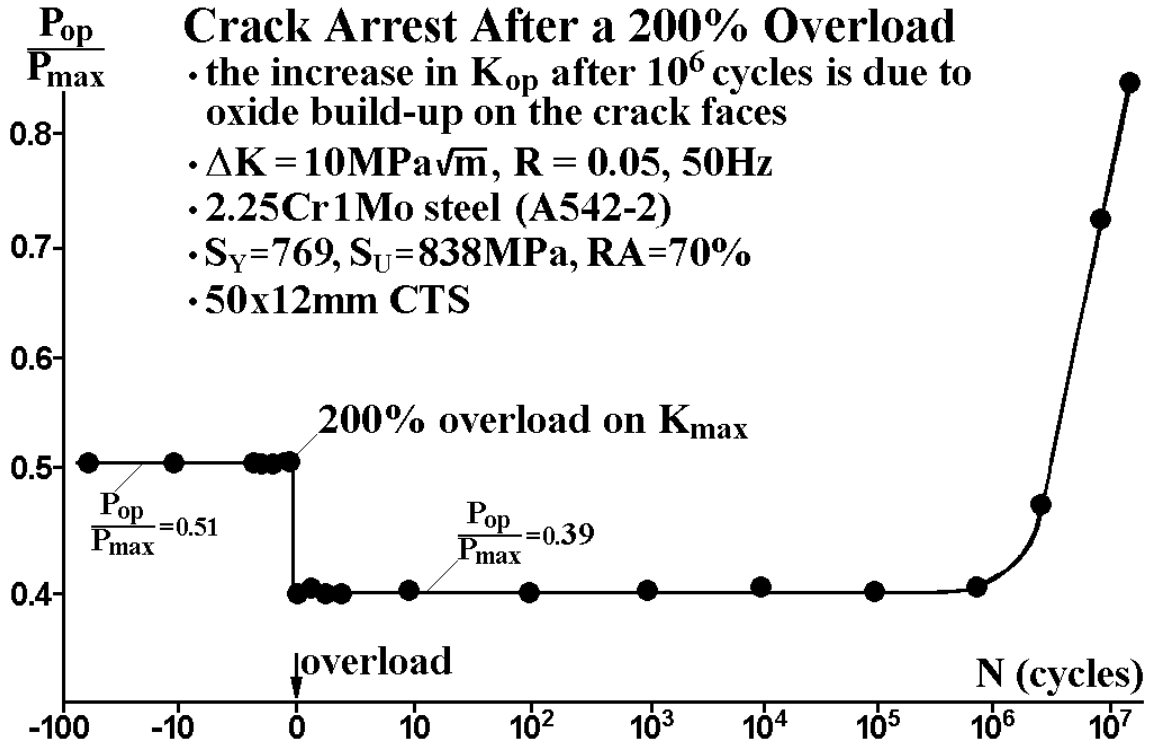

Fig. 16. Crack arrest associated with a 31% increase in ΔK_{eff}.

A final set of experimental results on crack retardation and/or arrest must be discussed. As expected from many of the crack closure models discussed above, no crack closure was detected in the **R = 0.7** FCG tests. Figure 17 presents some **P×ε** measurements before and after a 100% OL that arrested the crack, when it was growing at a baseline range $\Delta K_{BL} = 10MPa\sqrt{m}$. Exactly

the same behavior was observed in another specimen, this time with a ΔK_{BL} = **8MPa√m**, as shown in Fig. 18. Also, Fig. 19 presents similar results after a 50% OL which delayed the crack. Since no closure was observed neither before nor after any of these overloads (and, therefore, $\Delta K_{eff} = \Delta K$ during the entire tests), it can be concluded that at these high **R** ratios crack closure was not a suitable mechanism to explain load cycle interactions in FCG.

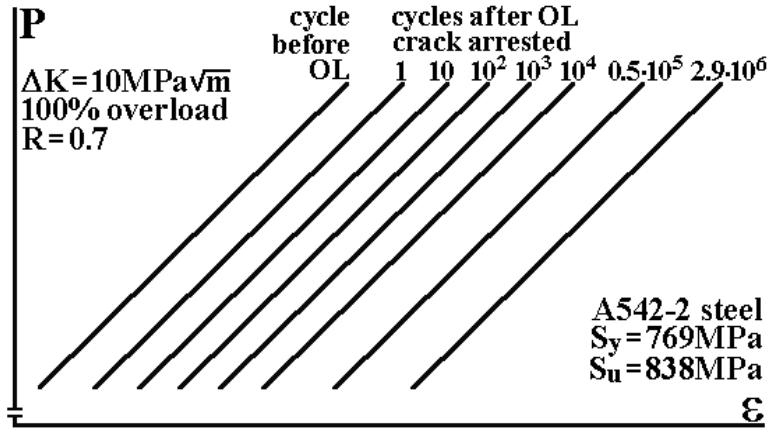

Fig. 17. **P×ε** measurements before and after a 100% OL that arrested the crack when it was growing at a ΔK_{BL} = **10MPa√m**.

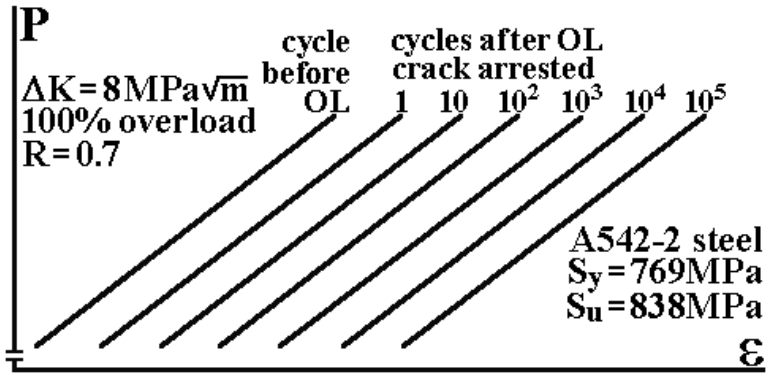

Fig. 18. **P×ε** measurements before and after a 100% OL that arrested the crack when it was growing at a ΔK_{BL} = **8MPa√m**.

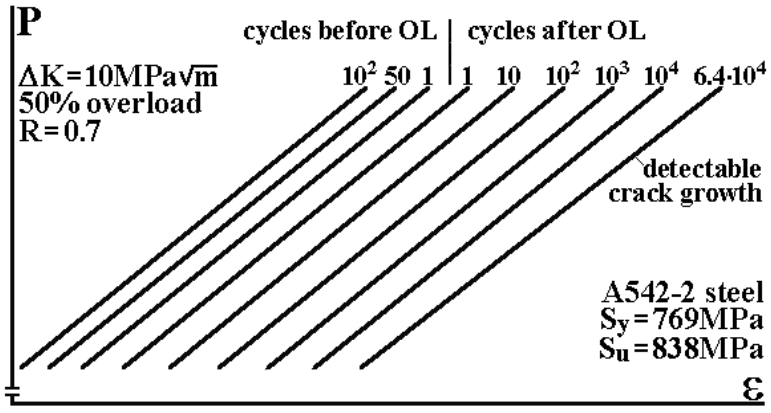

Fig. 19. **P×ε** measurements before and after a 50% OL that delayed the crack when it was growing at a ΔK_{BL} = **10MPa√m**. Note the change in the slope of the curve after the crack restarted to grow.

4. Conclusion

Fatigue crack closure is the most used mechanism to explain load cycle interactions such as delays in or arrests of the crack growth after overloads. Much work has been done in this field, and many researchers defend the idea that fatigue crack growth should be controlled by ΔK_{eff} and not by ΔK. However, closure concepts cannot be used to explain some interaction effects measured in plane-strain controlled fatigue crack growth. Therefore, the obtained experimental results indicate that the dominant role of crack closure in the modeling of fatigue crack growth should be reviewed.

References

[1] Paris P.C., Tada H. & Donald J.K. Service Load Fatigue Damage - a Historical Perspective. Int J of Fatigue 1999;21:S35-S46.

[2] Skorupa M. Load Interaction Effects During Fatigue Crack Growth under Variable Amplitude Loading - a Literature Review, Part 1: Empirical Trends. Fatigue and Fract of Eng Mat and Struct 1998;21:987-1006.

[3] Skorupa M. Load Interaction Effects During Fatigue Crack Growth under Variable Amplitude Loading - a Literature Review, Part 2: Qualitative Interpretation. Fatigue and Fract of Eng Mat and Struct 1999;22:905-926.

[4] Sadananda K., Vasudevan A.K., Holtz R.L., Lee E.U. Analysis of Overload Effects and Related Phenomena Int J of Fatigue 1999;21:S233-S246.

[5] Lang M., Marci G. The Influence of Single and Multiple Overloads on Fatigue Crack Propagation. Fatigue and Fract of Eng Mat and Struct 1999;22:257-271.

[6] Suresh S. Fatigue of Materials, Cambridge, 1998.

[7] Broek D. The Practical Use of Fracture Mechanics, Kluwer, 1988.

[8] Elber W. The Significance of Fatigue Crack Closure. ASTM STP 486, 1971.

[9] von Euw E.F.G., Hertzberg R.W., Roberts R. Delay Effects in Fatigue Crack Propagation. ASTM STP 513, 1972:230-259.

[10] Newman J.C. A Crack Opening Stress Equation for Fatigue Crack Growth. Int J of Fracture, 1984;24(3):R131-R135.

[11] Newman J.C., Crews J.H., Bigelow C.A., Dawicke D.S. Variations of a Global Constraint Factor in Cracked Bodies under Tension and Bending Loads. ASTM STP 1244(2), 1995:21-42.

[12] Castro J.T.P. A Circuit to Measure Crack Closure. Exp Techniques 1993;17(2):23-25.

[13] Ewalds H.L., Furnée R.T. Crack closure measurements along the crack front in center-cracked specimens. International Journal of Fracture, 1978;14:R53-R55.

[14] McEvily A.J. Current Aspects of Fatigue. Metal Science, 1977;11:274-284.

[15] Paris P.C., Hermann L. Fatigue Thresholds. EMAS, Warley, UK, 1982;1:11-33.

[16] Bernard P.J., Lindley T.C., Richards C.E. The effect of single overloads on fatigue crack propagation in steels. Metal Science, 1977;11:390-398.

[17] Schijve J. Fatigue of Structures and Materials. Kluwer Academic Publishers, 2001.

[18] Chang J.B., Engle R.M. Improved Damage-Tolerance Analysis Methodology. J of Aircraft, 1984;21:722-730.

[19] Forman R.G., Mettu S.R. Behavior of Surface and Comer Cracks Subjected to Tensile and Bending Loads in Ti-6AI-4V Alloy. ASTM STP 1131, Ernst H.A. et al eds., 1992:519-546.

[20] Schijve, J. The Stress Ratio Effect on Fatigue Crack Growth in 2024-T3 Alclad and the Relation to Crack Closure. Technische Hogeschool Delft, Memorandum M-336, 1979.

[21] Wang J., Gao J.X., Guo W.L., Shen Y.P. Effects of specimen thickness, hardening and crack closure for the plastic strip model. Theor. and Applied Fracture Mechanics, 1998;29:49-57.
[22] Kujawsky D. Enhanced model of partial crack closure for correlation of R-ratio effects in aluminum alloys. Int J Fatigue, 2001;23:95-102.
[23] Shih T.T., Wei R.P. A Study of Crack Closure in Fatigue. Eng Fract Mech 1974;6:19-32.
[24] Führing H., Seeger T. Dugdale Crack Closure Analysis of Fatigue Cracks under Constant Amplitude Loading. Eng Fract Mech 1979;11(1):99-122.
[25] Bachmann V., Munz D. Crack Closure in Fatigue of a Titanium Alloy. Int. J of Fracture, 1975;11.
[26] Kim J.K., Shim, D.S. The variation in fatigue crack growth due to the thickness effect. Int J of Fatigue 2000;22:611-618.
[27] Park H.B., Lee B.W. Effect of specimen thickness on fatigue crack growth rate. Nuclear Engineering and Design, 2000;197:197-203.
[28] Costa J.D.M., Ferreira J.A.M. Effect of stress ratio and specimen thickness on fatigue crack growth of CK45 steel. Theoretical and Applied Fracture Mechanics, 1998;30:65-73.
[29] Mills W.J., Hertzberg R.W. The effect of sheet thickness on fatigue crack retardation in 2024-T3 aluminum alloy. Engineering Fracture Mechanics, 1975;7:705-711.
[30] Saff C.R., Holloway D.R. Evaluation of crack growth gages for service life tracking. Fracture Mechanics (Roberts, R. Editor), ASTM STP 743, 1981:623-640.
[31] Schijve J. Fundamentals and practical aspects of crack growth under corrosion fatigue conditions. Proc. of the Institution of Mechanical Engineers, 1977;191:107-114.
[32] Shuter D.M., Geary W. The influence of specimen thickness on fatigue crack growth retardation following an overload. Int. Journal of Fatigue, 1995;17(2):111-119.
[33] Shuter D.M., Geary W. Some aspects of fatigue crack growth retardation behaviour following tensile overloads in a structural steel. Fatigue and Fracture of Engineering Materials and Structures, 1996;19:185-199.
[34] Suresh S. Micromechanisms of fatigue crack growth retardation following overloads. Engineering Fracture Mechanics, 1983;18:577-593.
[35] Castro J.T.P., Parks D.M. Decrease in Closure and Delay of Fatigue Crack Growth in Plane Strain. Scripta Metallurgica, 1982;16:1443-1445.
[36] Miranda A.C.O., Meggiolaro M.A., Castro J.T.P., Martha L.F., Bittencourt T.N. Fatigue Crack Propagation under Complex Loading in Arbitrary 2D Geometries. In: Braun AA, McKeighan PC, Lohr RD, editors. Applications of Automation Technology in Fatigue and Fracture Testing and Analysis, ASTM STP 1411(4), 2002:120-46.
[37] Castro, J.T.P. Some Critical Remarks on the Use of Potential Drop and Compliance Systems to Measure Crack Growth in Fatigue Experiments. Brazilian J Mech Sciences 1985;7(4):291-314.

[O6]

On the Specimen Thickness Effect on Fatigue Crack Growth

M.A. Meggiolaro, J.T. Pinho de Castro*, J.R. Durán
Pontifical Catholic University of Rio de Janeiro, Brazil

Plasticity-induced crack closure can have a very significant effect in the prediction of fatigue crack growth [1]. Neglecting this effect in fatigue life calculations can result in overly conservative predictions, increasing maintenance costs by unnecessarily reducing the period between inspections. In addition, some closure models predict that non-conservative predictions may arise from neglecting such effects. For instance, Newman [2] proposed that crack closure is not only a function of the load ratio **R**, but it is also dependent on the stress-state and on the maximum stress level. Assuming that plasticity induced closure is the only mechanism affecting crack propagation, the fatigue life of "thin" (plane stress dominated) structures is expected to be much higher than the life of "thick" (plane strain dominated) ones, when both work under the same stress intensity range and load ratio. Therefore, if **da/dN** curves are measured under plane stress conditions without considering crack closure, then the predictions on components under plane strain could lead to non-conservative errors as high as 75%, see Fig. 1. To avoid this error, it would be necessary to convert the measured crack growth constants associated with one stress condition to the other using appropriate crack closure functions. On the other hand, this thickness effect on **da/dN** is not recognized by the ASTM E645 standard on the measurement of fatigue crack propagation. In spite of mentioning the importance of crack closure, this standard only requires specimens sufficiently thick to avoid buckling during the tests. Recently, Kim and Shim [3] found that the variance of **da/dN** is increased in thin specimens of Al 7075-T6 alloy, but no significant thickness dependence of the average **da/dN** rates was reported. In this work, experiments are performed on CTS specimens with different thicknesses. Based on the measured **da/dN** rates, a study on the stress-state dependence of fatigue crack closure is presented.